On the sub-micron aerosol size distribution in a coastal-rural site at El Arenosillo Station (SW – Spain)

Mar Sorribas[1], Benito A. de la Morena[1], Birgit Wehner[2], Juan F. López[1], Natalia Prats[3,*], Sandra Mogo[4], Alfred Wiedensohler[2] and Victoria E. Cachorro[3]

[1] {'El Arenosillo' - Atmospheric Sounding Station, Atmospheric Research and Instrumentation Branch, INTA, Mazagón–Huelva, Spain}

[2] {Leibniz-Institute for Tropospheric Research, Leipzig, Germany}

[3] {Atmospheric Optics Group, University of Valladolid, Valladolid, Spain}

[4] {Department of Physics, University of Beira Interior, Covilhã, Portugal}

Correspondence to: M. Sorribas (sorribasmm@inta.es)

* Now at: Meteorological State Agency, AEMET, Canary Island, Spain

Abstract

This study is focused on the analysis of the sub-micron aerosol characteristics at rural and coastal environment in Southwestern Spain. Particle number size distributions were measured in the size range (14-673) nm using a Scanning Mobility Particle Sizer (SMPS, Model 3936 - TSI), from 15 July 2004 to 31 July 2006 at El Arenosillo Station. Mean total concentration was 8660 cm^{-3} and mean concentrations for the nucleation, Aitken and accumulation modes particles were 2830 cm^{-3}, 4110 cm^{-3} and 1720 cm^{-3}, respectively. Mean geometric diameters of the four modes particles, which characterized the mean size distribution per month, were about 16 nm, 42 nm, 103 nm and 237 nm. Two kinds of episodes produced a maximum of the total concentration around noon: the new particle formation and the regional recirculation such as the sea – land breeze. Two types of nucleation events (called N_1 and N_2) were observed. Events N_1 were an example of the influence of regional sources and Events N_2 showed the weight of local industries over the rural and coastal background levels. The 60% of nucleation events were related to NE and NW wind sectors (N_1 and N_2 respectively), a ΔT higher than 12 ºC, a wind speed higher than 2.3 m s^{-1} and a total surface area for the

accumulation mode particles below of 11190 μm^{-3} cm^{-3}. The influence of the sea – land breeze processes has been analyzed, observing increases of up to 50%, 110% and 90% of the particle concentration for the nucleation, Aitken and accumulation modes. Annual evolution of monthly averages allowed to conclude that the increase or decrease of 1 cm^{-3} of the concentration for nucleation mode particles was related to opposite trend of 0.5 cm^{-3} of the concentration for accumulation mode. This anti-correlation produced a weak seasonal evolution of the total particle concentration.

1 Introduction

The atmospheric aerosol plays an important role in the global understanding and regional climatic behaviour through their direct and indirect effects. According to Charlson and Wigley (1994), the concentration of natural aerosol has remained roughly the same since the industrial revolution, but human activity has increased the concentration of anthropogenic aerosol. The report of the International Panel of Climate Change (IPCC, 2007) claims that the effect of anthropogenic aerosol is uncertainly concerning their influence on the climate change. The direct effect of aerosol particles on climate is related to their absorption and scattering of solar radiation. The ratio of the scattering to the extinction coefficients describes the single scattering albedo and thus the influence of the aerosols on the radiation balance of the atmosphere (Takemura et al., 2002). The indirect mechanisms show the importance of the submicrometer particles as a potential source of cloud condensation nuclei (CCN), (Charlson et al. 1987).

During the last decade, the particle number size distribution has been measured in many places around the world (Heintzenberg et al., 2000; Kulmala et al., 2004) under different atmospheric conditions. Those measurements have been taken on different platforms (ground, ships or aircraft) and during short periods of time such as campaigns (Antilla et al., 2005; Dingenen et al., 2005; Mahajan et al., 2010), or long-term monitoring (Birmili et al., 2003; Tunved et al., 2003; Venzac et al., 2009). In this context, continuous background aerosol monitoring has been performed since 1996 at 'El Arenosillo'- Atmospheric Sounding Station, which is located in the southwest coast and rural area of Spain. To begin with, the efforts were focused in the characterization of the aerosol optical properties by means of remote sensing methods, using spectroradiometer and photometric measurements, (Vergaz et al.,

2005; Toledano et al., 2007a; Toledano et al., 2007b; Cachorro et al., 2008; Prats et al., 2008). In order to quantify the ~~incidence~~ of the tropospheric aerosol ~~over~~ columnar aerosol, in-situ monitoring of particle number size distribution was started in 2004. This paper presents the first ~~conclusions~~ of this aerosol ~~variable~~ within this framework. PM10 and PM2.5 mass concentrations have been widely analyzed in this area (Querol et al., 2004; 2008; Sánchez de la Campa et al., 2009) but there are not studies of the particle number size distributions.

This paper has the following sections: first, the area of study, the sampling station and the aerosol instrumentation, including its intercomparison with a GAW standard, are presented. ~~At~~ the result and discussion section, a statistical analysis of the size distribution over the course of two years is investigated, by means of the diurnal, seasonal and annual cycles of the total and modal concentration. The manual inspection of this evolution has ~~evinced the presence of~~ representative episodes with high particle concentration such as the new particle formation and the particle accumulation during sea-land breeze days, whose main characteristics are presented in terms of meteorological and aerosol physical parameters. This analysis is going to achieve the objective of this paper, since aerosol sources in a rural and coastal area such as the background environment of Doñana National Park will be assessed. Moreover, it will allow ~~to quantify the~~ influence of urban areas on the background monitored values.

2 Site, measurements and methods

2.1 Sampling station site

'El Arenosillo' - Atmospheric Sounding Station is a platform ~~to~~ investigate ~~some~~ topics ~~about~~ atmospheric sciences. One of the main research subjects at this station is the surface and remote sensing aerosol ~~study~~: from particulate mass levels (gravimetric) and chemical composition (Sánchez de la Campa et al., 2009), micrometer and sub-micrometer particle number size distributions (Sorribas, 2008) and integrating scattering and absorbing coefficients (Mogo et al., 2005; Mogo et al., 2010), to columnar aerosol physical and radiative properties (Toledano et al., 2007a). This station ~~was~~ equipped with instrumentation to measure other ~~different~~ atmospheric parameters, such as stratospheric ozone and UV solar radiation ~~together with their incidence~~ on biological ecosystem, ~~and presently is also capable~~

to monitor gaseous pollutant concentrations (O_3, NO_2 and NO_x) and meteorological parameters are also monitored.

This observatory is located at the Province of Huelva (37.1ºN, 6.7ºW, 40 m a.s.l.), among the Atlantic Ocean, Mediterranean Sea and North African, (see Fig. 1). It is situated at a rural protected environment, (Doñana National Park), which covers an extensive area with a homogeneous Mediterranean pine forest, and a coastal area at the south-west where the Atlantic Ocean seashore is at a distance less than 1 km. The nearest population is a small village, named Mazagón, about 8 km west direction. The biggest and closest population is the City of Huelva (160.000 inhabitants) at 35 km to the northwest. Emissions from industrial areas around Huelva could contribute to increase the background levels at the measured site for northwest winds.

The main aerosol types present at El Arenosillo Station are coastal marine, continental and desert dust. Air mass back trajectories with starting heights of 500 m a.s.l., were used to analyze the aerosol character and showed that the main component is represented by the coastal marine conditions, which present 44% of cases followed by continental aerosol air masses with an occurrence of 38% and finally desert dust air masses, that have a relevant frequency of 18% of data (Toledano, 2005). Moreover, desert dust events are more frequent during February-March and summer months (Toledano et al., 2007b; Prats et al., 2008; Córdoba-Jabonero et al., 2010).

The wind rose in the period (15/07/04 – 31/07/06) is presented in Fig. 1. The winds blew preferably from NE and SW, indicating air came perpendicular to the Atlantic coast line. It is seen the influence of atmospheric processes, such as the sea-land breeze, more common in spring and summer time with an occurrence probability of 30% in May and a maximum of 70% in August (Adame et al., 2008). Because of the sampling area is very flat, they can be considered as a mesoscale phenomenon. Furthermore, winds from Huelva City (NW) and its surroundings could be observed with lower occurrence.

About the main meteorological characteristics, the average ambient temperature oscillated between 26ºC in August and 12ºC in January (annual average = 19ºC). Wind speed ranges from less than 2.5 ms^{-1} in June to as high as 3.2 ms^{-1} in December (annual average = 3 ms^{-1}) (Adame et al., 2008).

2.2 Scanning Mobility Particle Spectrometer intercomparison

The dry ambient sub-micron particle number size distribution was monitored with a TSI Scanning Mobility Particle Sizer (Knutson and Whitby, 1975). In order to assess the quality of the measurements, an intercomparison of our system was carried out in the WCCAP (World Calibration Center for Physical Aerosol Research) in Leipzig (Germany). This Institute (IfT) is endorsed by the WMO within the framework of the GAW programme and it has designed a calibration program for maintaining and comparing the measurement instrumentation. In this investigation, the limitations of our system were analyzed with the aim to perform a correct interpretation of the results. It was achieved thanks to an intercomparison campaign held at the IfT from 8 to 10 December 2003. Some instrumental restrictions are the low efficiency for measuring the nucleation and Aitken modes due to the losses in the DMA inlet (Birmili et al., 1997) and in the CPC (Su et al., 1990).

The instrument of the IfT was a DMPS (Differential Mobility Particle Sizer), which is capable to measure the particle mobility diameter in the range of 7-400 nm. In the Electrostatic Classifier, the aerosols pass through a Kr-85 Bipolar Charger and a DMA type short-Hauke with a central electrode which length is 18 cm. The CPC Model used was the 3010 of TSI. The aerosol and sheath flows were 1.0 l min^{-1} and 10 l min^{-1} respectively.

The SMPS of El Arenosillo (TSI Model 3936) is made up of a differential particle size classifier (TSI Model 3080, Electrostatic Classifier), a Condensation Particle Counter (TSI Model 3022A) for particle detection and the AIM software (version 4.3, TSI INC., St. Paul., MN, USA) for data reduction and analysis of the SMPS output. The polydisperse aerosol flow was 0.3 l min^{-1} and the sheath flow was 3 $lmin^{-1}$, which was dried with silica gel in a closed loop.

Both spectrometers were connected to the same sampling system of atmospheric aerosol. Then, both instruments characterized the same air volume and the losses in the inlet and transport lines were the same. The measurements were carried out simultaneously every four minutes.

Hourly averages were calculated using both measurements and the DMPS - IfT size distributions were calculated in the SMPS - El Arenosillo diameters. The correction factor (CF) was calculated using the ratio of the same hourly averages of particle size distribution given by the SMPS - El Arenosillo and the DMPS - IfT, Eq. (1).

$$Correction\ Factor\ (D_i) = \frac{dN_i / d\log D_i\ (ElArenosillo)}{dN_i / d\log D_i\ (IFT)} \qquad (1)$$

In Eq. (1) the diameter dependence of this factor is observed. This CF allowed to make up for the losses that appeared in the SMPS, assuming as ideal instrument the characteristics of the DMPS of IfT. Fig. 2 shows the CF average and its standard deviation. For diameters smaller than 70 nm, a decrease in SMPS efficiency was observed, with a value of 50% in 20 nm. CF was 1 for particle sizes greater than 70 nm. Using this correction factor a good coincidence between both systems was observed.

2.3 Dataset

The surface aerosol measurements were carried out in a little home-laboratory, 75 m from the main building. The inlet was placed at 3 m above the forest and about 8 m above ground level. The aerosol sampling was obtained following the recommendations of Sheridan et al., (2001) with a flow rate of 330 $lmin^{-1}$ and Reynolds Number (*Re*) 9100, using a vertical stainless steel tube (48 cm inner diameter and 550 cm length). ~~Outer~~ tube was placed concentrically around the inner tube (1 cm inner diameter and 120 cm length), which introduced the sampling aerosol in the home-laboratory with a broad curve into the flow splitter. In this tube, the flow rate was 13.3 $lmin^{-1}$ and *Re* 1820. A conductive flexible tube with 0.6 cm inner diameter ~~connected to the flow splitter~~ transported the aerosol flow ~~up~~ to the SMPS instrument. Sampling system efficiency was calculated according to Willeke and Baron (1993) resulting an efficiency close to 85% for 16.5 nm particles. Sampling ~~effects~~ were corrected for data processing.

The sub-micron particle number size distributions were measured continuously with a time resolution of 10 min from 15 July 2004 to 31 July 2006. During this period there was one longer gap, from 25 July to 11 October 2005, due to some instrumentation failures. The SMPS was operational for 604 days (83%) and its maintenance was ~~made~~ according to the standard procedures. The ~~accuracy of~~ DMA size selection was tested with PSLs ~~obtaining a size resolution~~ lower than 2%.

All the spectra were checked to detect incorrect measurements and periods of rain influence. So, more than 75000 valid size distributions were obtained. The monthly number of measurements during the period of study is presented in Fig. 3, with about 3500-4000 spectra per month. ~~The data were prepared for processing using daily files~~. In this study, particle number size distributions were assumed to have a three modal structure: a nucleation mode (14–30 nm), an Aitken mode (30–100 nm) and an accumulation mode (100–673 nm).

183 Meteorological parameters were obtained at 0.5 km southwester sampling site.

184

185 ## 3 Result and discussion

186 ### 3.1 ~~Mean levels~~ Mode Descriptions

statistics for the total aerosol plus each of the modes

187 ~~In order to study the particle number size distribution,~~ Table 1 presents the mean total
188 concentration (N_T) with 8660 cm^{-3} ~~and the 10th and 90th percentiles with 3250 cm^{-3} and 15450~~
189 ~~cm^{-3} respectively.~~ The median value with 7090 cm^{-3} ~~is~~ indicating that the most frequent
190 values were smaller than the mean total concentration. ~~Another data-base recorded~~ ~~with the~~
191 ~~same~~ size range and in rural sites presented ~~mean levels such as~~: 16300 cm^{-3} in Pearl River
192 Delta (China) (Liu et al., 2008), 2210 cm^{-3} in Hyytiälä Station in southern central Finland
193 (Laakso et al., 2003) and 9280 cm^{-3} in Northern Italy (Ispra) (Rodríguez et al., 2005). ~~Thus~~,
194 the particle concentration at El Arenosillo was closer to the measured levels in rural areas,
195 located to similar latitudes in Europe.

with only 3 points of comparison this is a somewhat sweeping generalization I would say ARN falls in middle

196 ~~About~~ modal concentrations, the mean values were 2830 cm^{-3}, 4110 cm^{-3} and 1720 cm^{-3} for
197 the nucleation (N_{NUC}), Aitken (N_{AIT}) and accumulation (N_{ACC}) modes respectively, (see Table
198 1). Standard deviation of N_{NUC} represented a variation of 100%, while N_{AIT} and N_{ACC} ~~was~~
199 higher than 65%. There is not a long-term monitoring of the aerosol particle size distribution
200 conducted in rural areas in Spain. But if levels at El Arenosillo Station were compared to
201 other rural sites in Europe, N_{NUC} was higher than those over continental area such as Northern
202 Italy (Rodríguez et al., 2005) while it is lower than levels observed during spring time in
203 Hyytiäla Station (Laakso et al., 2003). On the other hand, similar concentrations for three
204 modes were observed at the Melpitz Station, when air mass type was Southern continental
205 (Birmili et al., 2001).

206 In Fig. 4a the relative occurrence frequency for mode diameter (size corresponding to
207 maximum concentration) for ~~1-hour data-base~~ is presented. ~~In this way~~, the variability due to
208 changes ~~for the~~ number density ~~was removed~~ and the shape of the mean distribution ~~could~~ be
209 analysed. The main features of the Fig. 4a show a high variability of the mode diameter
210 within a wide range, 16.5 – 143 nm, with two maximums of 22% for 16.5 nm and 11% for
211 69.8 nm. N_T was distributed around mean value of 8660 cm^{-3} (see Table 1) as Fig. 4b shows,
212 ~~finding~~ the higher frequency ~~with~~ 18% at 6000 cm^{-3}, ~~and there was~~ only 1% of total
213 concentration above 24000 cm^{-3}.

The biggest forest fire of the last decades happened at the North of Huelva Province, from 27 July to 4 August 2004. The smoke plume reached up to El Arenosillo Station, adding fine aerosol particles and affecting atmospheric conditions. During these days, the area also suffered the most intense desert dust intrusion (22 July – 4 August), ever registered during the last years with modern photometric techniques (for details see Cachorro et al., 2008; Prats et al., 2008). In this present study the union of these two events is named 'mixed event'. Unfortunately, problems occurred with the SMPS system during the period 24-27 July, making it impossible to realize a detailed analysis of his beginning.

In order to understand the annual behaviour of the total and modal particle number concentration and the impact of this special event over mean values, Table 1 lists the statistical parameters during the entire period of study and only during the 'mixed event'. During this episode, mean total particle number concentration was about 3.2 times higher than that usually encountered and his maximum was more than 188000 cm^{-3}.

In general, the particle emissions from forest fires are dominated by an accumulation mode, (Niemi et al., 2004; Janhäll et al., 2010) and occasionally also by a nucleation mode caused by the gas-to-particle conversion of inorganic and organic species released during the plume aging (Reid et al., 2005). In the 'mixed event', the mean concentration for nucleation, Aitken and accumulation modes increased by the factors of 4.7, 2.9 and 1.3 respectively and then, nucleation mode was the most influenced. Because of ultrafine mode changes fast and is not transported in the atmosphere as far as accumulation mode particles, these results can also indicate the closeness of the place where this event occurred (only 70 km away). The frequency of some aerosol physical properties for the mixed event is clearly seen in Fig. 4b, with ~30% of data below 9000 cm^{-3}, and ~43% above 24000 cm^{-3}. On the other hand, Fig. 4a shows the highest incidence over the smallest diameters with ~40% for 16.5 nm.

3.2. Monthly and seasonal total and modal concentrations

The daily number concentration average was evaluated using the hourly averages and the 75% quality criteria. For example, a day that represented a high daily average value was 11 April 2005 with 16532 cm^{-3}, during which the presence of a nucleation event increased the particulate levels at midday. The predominance of the accumulation mode during all day, allowed to chosen the 20 January 2005 as example of a day with a similar concentration to the mean level, with 7940 cm^{-3}. Finally, 11 May 2005 was selected as representative of a low

concentration, with 2520 cm^{-3}. During the day before, it was drizzling and thus, the daily concentration average during 11 May was representative of the wet deposition conditions.

Fig. 5 shows the monthly averages of the total and modal particle number concentrations, calculated using daily averages. 10th and 90th percentiles are indicated in subplots, showing a high daily variability for the number concentration. The maximum was obtained in July 2006 with 11300 cm^{-3} and the minimum in January 2005 with 6830 cm^{-3}. The mean total and modal concentrations are also represented (dashed grey line in Fig. 5 and also see Table I).

In Fig. 5b and 5d, the monthly N_{NUC} and N_{ACC} are plotted and some periods are chosen to study in detail the behaviour between both concentrations (see grey areas). As it is showed the Periods A (January - March 2005) and B (April - June 2005) are representative of a clear anti-correlation between N_{NUC} and N_{ACC}, observing an increase/decrease of N_{NUC}/N_{ACC} respectively during the Period A and an opposite behaviour during the Period B.

The Period A showed an increase of N_{NUC} with a rate of 570 cm^{-3} month^{-1} and a decrease of N_{ACC} with 230 cm^{-3} month^{-1}. Also, 60% of the particles in the nucleation mode grew to Aitken size range, increasing N_{AIT} with a rate of 340 cm^{-3} month^{-1}. This behaviour may be related to the new particle formation, a process which is promoted with a reduction of N_{ACC} and an increase of N_{NUC} and N_{AIT}, as it has been observed.

And during the Period B, N_{NUC}/N_{ACC} decreased/increased with a rate of 570/300 cm^{-3} month^{-1} respectively. This could be explained to the presence of large particles from desert dust air mass and from an increase of atmospheric stagnation which resulted in an aerosol aging and therefore an increase for N_{ACC}. Higher N_{ACC} produced a large surface area concentration which favoured the condensation of gases onto pre-existing particles and suppressed the new particle formation (decreasing N_{NUC}). Both processes are present over the Iberian Peninsula during the Period B and during spring-summer time in general (Toledano et al., 2007b; Querol et al., 2008).

If the trends of N_{NUC} and N_{ACC} during the Periods A and B are compared, it is possible to conclude that the decrease/increase in the accumulation mode of 0.5 cm^{-3} is related to an increase/decrease in the nucleation mode of 1 cm^{-3}.

On the other hand, the great variability among the same months on several years is striking, such as the comparison between the concentration evolutions during Period B and Period C (April – June 2006) evinces. Thus, in April 2005 and 2006 there were a mean values with

4040 cm^{-3} and 2710 cm^{-3} (1.5 times lower) respectively for N_{NUC} and with 1220 cm^{-3} and 1940 cm^{-3} (1.6 times higher) for N_{ACC}. It ~~can be~~ related to the trend toward ~~the increment of~~ the desert dust episodes observed since 2002 (Toledano et al., 2007b).

From the ~~evolution of the data-base~~, a trend ~~toward the increment~~ of N_{AIT} with a rate 1150 cm^{-3} year^{-1} was observed, such as the correlation line shows in Figure 5c. It is not possible to indicate the reason for this behaviour, since it would take many more years with measurements. ~~The anti-correlation between N_{NUC} and N_{ACC} produced a weak annual cycle of N_T, marked principally by increasing N_{AIT} (see correlation line in Figure 5a).~~ The non-dependence of N_T with the season is a behaviour not observed in other rural background areas, which usually shows a clear maximum during summer time (Laakso et al., 2003; Ström et al., 2003; Venzac et al., 2009). In contrast, other *in-situ* compounds such as tropospheric ozone at El Arenosillo station exhibits an increase of 50% for its concentration from winter to summer times, (Adame et al., 2010).

An often applied approach is the use of equations to describe the size distribution as separated modes, *i.e.*, as lognormal aerosol size distribution. This technique was applied over the mean size distribution per month which was lognormal fitted in four modes. The average geometric mean diameter (GMD) observed at El Arenosillo, was about 16 nm, 42 nm, 103 nm and 237 nm, respectively for the nucleation, Aitken, accumulation 1 and 2 modes. Typical continental environments show normally only one accumulation mode which presents a GMD greater than 150 nm (*e.g.* Birmili et al., 2001, Tunved et al., 2003; Venzac et al., 2009). This accumulation 2 mode was made up to larger particles and it could be related to the presence of the desert dust events over the Iberian Peninsula.

3.3. Diurnal evolution of the modal size ranges

The diurnal evolution of the total and the modal particle number concentrations were calculated from hourly averages for each month. The mean diurnal cycles of N_T, 10th and 90th percentiles are indicated in Fig. 6a and of N_{NUC}, N_{AIT}, and N_{ACC} in Fig. 6b. Higher values for N_T were found during day time because of an increase ~~for~~ in N_{NUC} and N_{AIT}, ~~being~~ with the maximum concentration occurring around noon. As Fig. 6a shows, the 90th percentile is the most appropriate statistic parameter to observe this tendency.

The highest values for N_{NUC} were observed in April 2005 and in July 2006 with 10200 cm^{-3} at 12:00 GMT and 10:00 GMT respectively. The maximum for N_{AIT} was found in July 2006

with 10850 cm^{-3} at 11 GMT. The lowest values for N_T were reached during the early morning hours with round 5500 cm^{-3}. They were observed as much winter (January 2005) as summer (July 2005) months. This again shows the enormous variability of the ultrafine particle concentration founded at El Arenosillo. These main reasons will be presented in Section 3.4.

Fig. 7 shows the daily mean cycles per season for the total and modal concentrations which were calculated from the daily mean cycles per month (more details in Fig. 6). Nucleation and Aitken modes governed the daily behaviour during spring-summer times. During winter-autumn times the daily evolutions were determined only for the nucleation mode. The maximum for N_{NUC} were reached at 11:00 GMT and 10:00 GMT and for N_{AIT} at 11:00 GMT during spring and summer times respectively. Then, during summer time there was a delay of 1-hour between the maximum for N_{NUC} and N_{AIT}.

This observation asserts that the particle growth rate was higher during the spring months. This may be due to during spring time, the pollination of the forest around El Arenosillo was at the height of the VOC's emissions to the atmosphere. Moreover, the particle area surface was lower in spring than in summer time, because of the number of desert dust episodes was also lower. They could allow the condensation process over the new particles was more efficient and thus, the particle growth rate in spring was higher than summer time. On the other hand, the colder seasons (autumn and winter) had their maximums for N_{NUC} at 14:00 GMT and 13:00 GMT respectively and for N_{AIT} was during night-time.

The decline for N_{NUC} and N_{AIT} in the afternoon was faster during summer time than spring time. Moreover, summer time presented in the late afternoon an increase of concentration for all of the particle sizes. Maybe, at night time the VOC's concentrations were higher than during day time, in spite of lower emissions, due to the shallower and more stable nocturnal boundary layer (Ieda et al., 2006). It could produce a particle growth by coagulation of small particles and by condensation of volatile organic components over pre-existing particles (Kulmala et al., 2001; Rodríguez et al., 2005), and then to explain the increase for N_{NUC} and N_{AIT} in the late afternoon.

Moreover at night, the minimum levels for N_T during the cold seasons were 15% lower than warm months, and it could be due to an increase of the atmospheric mixing and then the dilution processes with respect to spring and summer times. About the absent of the diurnal evolution of N_{ACC}, its composition by long-lived particles must be taken into account and then

it can explain that it not disappear and reappear in a diurnal behaviour, (Rodriguez et al., 2005; Venzac et al., 2009). Need to be careful comparing w/PDD - mountain sites have diff diurnal drivers

With the aim to study the relation between different particle size ranges, the linear correlation coefficients between hourly N_{NUC}&N_{AIT} (R = 0.40), hourly N_{AIT}&N_{ACC} (R = 0.38) and hourly N_{NUC}&N_{ACC} (R = 0.09) were calculated. As expected, ~~concentration for~~ diurnal cycles in N_{NUC}&N_{AIT} and N_{AIT}&N_{ACC} were statistically dependent on each other ~~in a daily behaviour (hourly tendency),~~ by the previous mentioned processes such as nucleation, condensation and coagulation. What is surprising is ~~when~~ that the correlation N_{NUC}&N_{ACC} ~~is evaluated from~~ for daily and monthly averages ~~since~~ increasing to R = 0.33 and R = 0.66 respectively. Then, the ~~relationship~~ anti correlation between these two modes is observed again, as was showed in Section 3.2, when long-term scale was used.

3.4. Study of representative episodes

If there is no strong synoptic forcing, the coastal areas are influenced by mesoscale processes because of the diurnal heating and cooling differences between the land and sea. In an area ~~as~~ like El Arenosillo, it determines the regional atmospheric conditions which affect the re-circulation of aerosol particle emitted by local and long-transport sources. ~~The manual~~ The inspection of daily evolution of the particle size distribution ~~and~~ in conjunction with the wind direction allowed ~~to~~ for distinguish ~~two episodes of interest with~~ identification of two types of high particle number concentration events: the first, related to the sea-land breeze days and the accumulation of the pollution in the wind flow; and the second, to the new particle formation by nucleation processes. ~~These last ones~~ nucleation events were observed as much under breeze re-circulation as synoptic forcing.

With the aim to present the main properties of the particle size distribution, initially each day was classified on the basis of the sea-land breeze phenomenon and for which, the methodology used in Adame et al., (2010) was applied. Then, all data-base (604 days) was separated in 106 days (18%) and 498 days (82%) with and without atmospheric re-circulation, respectively. The classification scheme can be observed in Fig. 8. Adame et al., (2010) ~~evinced~~ identified the existence of two different sea-land breeze patterns, called pure-breeze and non-pure breeze. In our work, the differences in both patterns ~~will~~ are not explain because they were presented in great detail in ~~the previous mentioned paper. Just with the aim to show the importance of the~~ Adame et al (2010) Fig 9 of wind direction depending of sea-land breeze type, ~~Fig. 9 can be observed. So, as long as~~ The land breeze flow for pure breeze is blowing from NE (Doñana National Park and Seville

move to after this sentence

Should say a little bit more about pure relate to pollution or flow parameters.

City), it is from NW (Huelva industrial areas) for non-pure breeze. Fig. 1 ~~situates better these~~ shows these different particle sources regions. In our data-base, the 106 days influenced by sea-land breeze can be segregated in 51 days (8%) for pure breeze type and in 55 days (9%) for non-pure breeze type. The percentages showed in brackets in this section are ~~referred to~~ in reference to the 604 days of the entire data-base.

~~With regard to~~ Nucleation events, which will be characterized in more detail in later sections, have been classified into two types depending on the wind direction during the ~~previous~~ hours prior to ~~of~~ the nucleation burst ~~particles~~: Event N_1 is if the wind was coming from NE and N_2 is if was from NW. The nucleation events were not observed in the remaining wind sectors. N_1 and N_2 episodes were detected under the breeze and non-breeze patterns and ~~then, its~~ their occurrence has been evaluated for each ~~one~~ breeze pattern (see Fig. 8). As no differences were observed between ~~both~~, these breeze & non breeze events patterns have been combined and Event N_1 occurred for 48 days (8%) and Event N_2 for 42 days (7%), as Fig. 8 shows.

If the days with Events N_1 and N_2 are removed ~~on~~ from the classification of non-breeze and breeze days, 48 days (8%) were representatives of pure breeze pattern (PB days), 36 days of non-pure breeze pattern (N-PB days) and 430 days of no breeze pattern (71%). These will be discussed in detail below.

3.4.1. New particle formation events (N_1 and N_2)

Fig. 10 shows some selected examples of the different short time events. The evolution of N_{NUC}, the total area surface concentration (S_T), ~~as well as~~ and the wind direction ~~can be~~ are also ~~observed.~~ shown The first short time event analysed was due to the new particle formation by gas-to-particle conversion. Three nucleation events with different characteristics are showed in Fig. 10a, 10b and 10c which appeared during 11 April 2005, 8 June 2005 and 18 December 2004 respectively. ~~Theirs main~~ The properties were calculated using the methodology presented in Birmili et al., (2003). The first ~~one~~ event started at 09:30 GMT and it had a total duration of 19.2 h, a particle formation rate of 3.5 cm^{-3} s^{-1} and a growth rate of 3.8 nm h^{-1}. ~~But~~, The second one started at 08:50 GMT and it ~~was~~ had a lower duration (6.8 h) and formation rate (2.4) ~~with 6.8 h and 2.4 cm^{-3} s^{-1}~~ than the first event respectively, ~~being~~ but its growth rate higher with 5.3 nm h^{-1}.

The homogeneous nucleation process enhanced the particle concentration at diameters below the detection limit of our particle spectrometer. The growth toward greater diameters, due to the condensation and coagulation processes, caused an increase of number concentration, at

first for the nucleation mode and later, for Aitken and accumulation size ranges, ~~such~~ as the evolution of mode diameter evinces in Fig. 10a and 10b. The 'banana' shape ~~representative~~ for these two events allows determining that these events were produced simultaneously in ~~a~~ large area (at least 100 km). So, new particles ~~which are~~ formed ~~in other~~ point are growing during the transport to El Arenosillo site and theirs sizes were measured ~~within~~ of the ~~ultrafine~~ mode. ~~Due to the~~ sampling size started at 14 nm, it is not possible to conclude that the formation processes took place in the sampling site. These two nucleation events were characterized by a slow increase of S_T and by a fast increase and later decrease of N_{NUC} with the maximum around midday.

Meteorological analysis showed that they occurred when the wind was blowing from the NE direction during the prior hours ~~of its apparition~~, (see Fig. 10a and 10b). ~~They have been called Event~~ N_1. ~~This is followed by a study on the place where this new particle formation was produced, choosing as example~~ the day 11 April 2005. ~~Given that~~ the initial size of the new particles was 1 nm, the lowest diameter measured in El Arenosillo was 14 nm and the growth rate was 3.8 nm h^{-1}, the formation occurred 3.7 h before that the particle arrived to the sampling site. ~~Then, it happened at~~ 05:50 GMT. ~~During that time~~, ~~while the new particles arrived at~~ El Arenosillo, the average wind speed was 4 m/s, ~~which allows to conclude~~ that the first monitored particles were formed as ~~very~~ close to 55 km away in NE sector. Due to the changes in the wind direction occurred after 12:00 GMT, the particles that previously passed on El Arenosillo during the morning are again measured in the afternoon. ~~Given that they had~~ grown ~~through~~ the condensation and coagulation processes, ~~it was~~ possible to observe ~~a~~ nucleation event ~~so long~~.

In Fig. 11a ~~the~~ median diurnal evolution of the particle number size distribution for the 48 days (see Fig. 8) ~~with presence of~~ Event N1 ~~is presented~~.

~~Selecting the PB~~ days and those with the wind blowing ~~from the NE direction during all day~~, ~~in~~ Fig. 12 are presented the main characteristics of the ~~daily mean~~ of the particle concentration ~~by means of~~ some aerosol physical properties and some meteorological parameters. The daily mean properties for all days are in black ~~colour~~ and the days with Events N_1 are presented in red ~~colour~~. Fig 12a shows an anti-correlation between N_{NUC} and total area surface concentration for accumulation mode (S_{ACC}), while in contrast, N_{ACC} & S_{ACC} and S_T & V_T are highly correlated (see Fig.12c and Fig. 12d). The Events N_1 ~~(red spots)~~ are associated to low

or medium values of S_{ACC}, N_{ACC} and V_T. It is due to the presence of pre-existing particles provides enough area surface to use the precursor gases in the condensation process and then to increase the size but no the particle number in the atmosphere. Then, these gases are not used in the nucleation processes.

N_{NUC} is also represented by means of some meteorological factors such as ΔT (temperature difference between minimum and maximum every day) and wind speed, (see Fig. 12e and 12f respectively). ΔT is related to the mixing status of the atmosphere. Since, higher values of ΔT are representatives of better mixing. In Fig. 12e, it is evinced that the Events N_1 were produced with ΔT above 10 ºC. This observation was already realized in Buzorius et al., (2003) where, it was concluded that days with new particle formation appeared with advection of cold air toward surface and then with high values of ΔT.

Finally, Fig. 12f showed Events N_1 occurred when the wind speed was higher than 2 m s^{-1} and the highest N_{NUC} was reached during the highest speed averages.

In order to propose a methodology for the quantification of the aerosol physical properties and meteorological parameters which are necessary for predicting the Events N_1 at the southwest Spain, some statistical parameters have been evaluated. Then, the conclusions have been that 60 % of Events N_1 can be predict if the wind is blowing from the NE direction in the morning and there are a S_{ACC} below of 11190 μm^2 cm^{-3} (30^{th} percentile), a ΔT higher than 12 ºC (10^{th} percentile), and a wind speed higher than 2.3 m s^{-1} (10^{th} percentile).

Particle number size distribution evolution during 18 December 2004 is chosen as an example (see Fig. 10c) to display the second type of nucleation event. These events happened when the wind was blowing from NW-N directions. They could be explained as a secondary particle formation which was produced by the emissions from the industrial areas situated around Huelva City. Because of the wind effects, the anthropogenic pollution with a continuous high level of precursor gases can be able to cause an increase of the concentration for ultrafine size range over the sampling site during an elapsed time between 2 and 8 hours.

It was called Event N_2 and it is also different than the analyzed previously, because the highest plateau concentration of N_{NUC} was maintained over time. So, N_{NUC} in Fig. 10a and 10b present a slight diurnal trend toward the larger particles sizes, which was characteristic of the Event N_1, while in Fig. 10c the maximum of N_{NUC} stays longer during the Event N_2. It can be explain because the particle source of the Event N_1 could be a large area and, in function of

463 ~~the time that the particle took to arrive at El Arenosillo, it could have grown up to different~~
464 ~~diameters~~. However, in the case of the Event N_2, it could be a ~~punctual~~ source ~~and then~~ all
465 particles emitted simultaneously ~~were~~ arriving at El Arenosillo at the same time ~~and they were~~
466 grown up to similar size.
467 ~~Otherwise, they were~~ characterized by an increase of S_T only during the last hours of the
468 episode. ~~About the relation of Event~~ N_2 ~~with the~~ aerosol properties and the meteorological
469 factors, ~~they were~~ similar to those observed for the case of Event N_1 in Fig. 12.
470 diurnal evolution of the particle number size distribution for the 42 days with presence of
471 Event N_2 (see Fig. 8) is presented in Fig. 11b.
472 Fig. 13 shows the number of the events per month (N_1 and N_2). ~~With the aim to evident the~~
473 ~~representatively of the results~~, the number of measured months is also indicated. The Event
474 N_1 presented a clear seasonality with two maximum (in March and in December) of 5 and 4
475 events per month respectively. The minimums were reached during summer time, ~~being its~~
476 ~~occurrence~~ zero during July and August. ~~Just as, it has commented at some opportunities~~
477 ~~throughout this report~~, this behaviour could be related to ~~the increment of the~~ desert dust
478 episodes during summer time. ~~On the other hand,~~ the monthly evolution of the Event N_2 (see
479 Fig. 13), did not show a clear behaviour.

480 3.4.2. Sea-land breeze days

481 The presence of regional re-circulations ~~as~~ the sea-land breeze are very typical over the
482 coastal areas during spring and summer time and they play an important role in transporting
483 air pollution from and towards the urban areas, (Ma and Lyons, 2003; Sorribas et al., 2007;
484 Adame et al., 2010; Wright et al., 2010). As noted above in Section 3.4, two types of sea-land
485 breeze over our study area have been observed: pure breeze and non-pure breeze. Wind
486 blowing at night from the land (NE for pure breeze and NW for non-pure breeze) towards the
487 sea as a result of the nocturnal cooling of the land surface is called land breeze. This local
488 wind produced an accumulation of particles ~~over the sea at~~ offshore ~~distance~~. ~~Then~~, the wind
489 direction changed at round 07:00 GMT and 08:00 GMT for pure breeze and non-pure breeze
490 respectively (Fig. 9a). It ~~was~~ blowing during the day from the sea ~~surface~~ (SW sector for both
491 land patterns) towards the land as a result of diurnal heating of the land surface (sea breeze).
492 Then, the accumulated particles ~~was~~ transported ~~over the~~ land, increasing the background
493 levels.

Fig. 14 shows the mean daily particle number size distribution and mean daily evolution of modal concentrations corresponding to 430 NB-days, 48 PB-days and 36 N-PB-days (see the day segregation in Fig. 8). 10th and 90th percentiles are also represented.

To quantify the effect of each type of breeze, due to the accumulated particles ~~at~~ offshore distance, NB days were chosen as reference of the modal concentration ~~reached~~. For NB days, the maximum concentration of N_{NUC} (N_{NUCmax}) was 3450 cm^{-3} (Fig. 14b.1). It was a 30% for PB and a 50% for N-PB days ~~higher~~ than for NB days (Fig. 14b.2 and 14b.3). ~~In the case of~~ N_{AITmax}, during NB days ~~its level~~ was 4280 cm^{-3} and for PB and N-PB it was 30% and 110% higher respectively (Fig. 14c.1, 14c.2 and 14c.3). And finally, N_{ACCmax} was 2000 cm^{-3}, increasing by 90% for PB days and decreasing by 5% for N-PB days (Fig. 14d.1, 14d.2 and 14d.3). ~~Then~~, it is concluded that the two breeze patterns were a particle source ~~within~~ the ultrafine size range and ~~only PB scenario within~~ the accumulation mode. ~~Some factors that has to be taken into account are~~ that PB days ~~were~~ influenced by continental air mass (see Fig. 1 and 9a) and ~~then~~, the ~~size range more influenced was~~ the accumulation mode. ~~On the other~~ hand, marine and industrial aerosol had an influence on the concentrations measured during N-PB days, ~~which have a size within the~~ ultrafine range.

For PB days, the daily evolution of N_{NUC} presented three minimums (Fig. 14b.2), which were reached at 08:00 GMT, 18:00 GMT and 02:00 GMT. This behaviour was only observed in this scenario. The first minimum may be caused by the mixing processes that ~~could~~ begin after sunrise and ~~therefore the~~ breakdown of the mixed layer, ~~which~~ increased the particle dilution. And the second and third minimums and the maximum concentration at 20:00 GMT had already been discussed earlier in Section 3.3 due to the evolution of N_{NUC} and N_{AIT} observed in Fig. 7 during the summer months. During these months, the occurrence of the breeze phenomenon is higher as the maximum gradient of temperature between land and sea is reached. ~~Thanks to the evolution shown in~~ Fig. 14b.2, ~~it is reasoned~~ that the behaviour ~~can~~ be observed in Fig.7 is only caused by the PB scenario. Future ~~woks~~ will be ~~guided to know~~ the reason for this behaviour, ~~which will be based on the correlation to some~~ meteorological parameters with vertical resolution and the aerosol data.

The evolution of N_{NUC} during N-PB days presented an absolute maximum at 10:00 GMT, ~~then~~ two hours before that PB days (Fig. b.2 and b.3). This behaviour could be related to the ~~transport~~ particle speed (wind speed), which for N-PB days is generally higher (see Fig. 9b).

~~As long as the~~ while the maximum concentration at noon for N-PB and PB days was due to the accumulated particle produced by the land breeze, the maximum concentration for NB days ~~was because of the occurrence of episodes similar than Events N_1~~ recirculation of is attributed to Event N_1 episodes. The difference between the mean size distribution of Event N_1 (Fig. 11a) and the mean total particle concentration of NB days (Fig. 14b.1, 14c.1 and 14d.1) was the maximum of the total particle concentration reached. Thus, for the case of Event N_1, that maximum was greater than 17000 cm^{-3} and for the case of NB days was around 10000 cm^{-3}.

On 15 September 2004 has been selected as example of an N-PB day (Fig. 10d). The wind direction evolution shows that land breeze propagated in offshore direction (from NW-N) during the night, the onset of sea breeze was at 09:30 GMT and then the sea breeze blew perpendicular to the coast (from SW). 40 minutes later, an air mass with high particle concentration came to the sampling area ~~and it was~~ influencing the site during the next five hours. Concentrations ~~were multiplied~~ increased by 12, 3.8 and 2.6 for the nucleation, Aitken and accumulation modes, while the polluted air mass was sampled. Total surface concentration ~~was~~ also increased. This event was the longest observed of its type? during the data-base analyzed. During the DAMOCLES campaign, these type of episodes were also differentiated using PM and chemical composition measurements over this area, (Pey et al., 2008).

4. Conclusions

In this paper, an analysis ~~about~~ of the sub-micron particle number size distribution in Southwest Spain is presented. ~~It was~~ size dist were measured continuously during 604 days at El Arenosillo Station which is located in a rural and coastal background environment. Mean total concentration was 8660 cm^{-3} and mean modal concentrations were 2830 cm^{-3}, 4410 cm^{-3} and 1720 cm^{-3} for N_{NUC}, N_{AIT} and N_{ACC} respectively. The most significant episode was a 'mixed event' of a strong desert dust intrusion plus a forest fire occurred during 27 July – 4 August 2004. It increased the mean modal concentrations by 4.1, 2.8 and 1.2, respectively.

~~About the modal parameters~~ the mean size distribution ~~per month~~ was separated in four modes and the mean geometric diameters were about 16 nm, 42 nm, 103 nm and 237 nm for nucleation, Aitken, accumulation 1 and accumulation 2 modes, respectively. again are these for entire database or monthly avg or?

Daily pattern concentrations exhibited an absolute maximum of the total concentration around noon, which was governed by N_{NUC} and N_{AIT} during the warm seasons and ~~only~~ by N_{NUC} during cold

seasons. This maximum was produced for the new particle formation and for the accumulation of particle during the typical air mass recirculation over the coastal areas such as the sea - land breeze. By means of the wind direction, two types of nucleation events (called N_1 and N_2) were detected. 60% of these were related to NE and NW wind directions respectively, a S_{ACC} below of 11190 μm^2 cm^{-3}, a ΔT higher than 12 ºC and a wind speed higher than 2.3 m s^{-1}. Events N_1 were an example of the influence of regional sources and they were characterized by the aerosol number transfer from the nucleation to the Aitken mode due to particle growth. However, Events N_2 showed the weight of local industries over the rural and coastal background levels and they did not evince the particle size growth. The number of Events N_1 per month presented the maximum values during spring and winter with 5 and 4 events respectively and the annual evolution could be related to the frequency of desert dust episodes. The monthly evolution of the Events N_2 did not show a clear behaviour.

The influence of the sea – land breeze processes has been presented by means of two different patterns (pure and non – pure breezes), observing that both were particle sources within ultrafine size range. If the maximum particle concentrations for NB days are chosen as reference (3450 cm^{-3}, 4280 cm^{-3} and 2000 cm^{-3} for N_{NUC}, N_{AIT} and N_{ACC} respectively), N_{NUCmax} was increased about 30% and 50% for PB and N-PB days respectively, and N_{AITmax} about 30% and 110% respectively. N_{ACCmax} was only increased about 90% for PB days.

Because Events N_1, Events N_2 and the N-PB and PB days were well determined from the wind sectors, the horizon of the sampling site could be divided into two hemispheres. High particle number concentration hemispheric (HC) from SW to NNW in clockwise presented (9120 ± 264) cm^{-3} and lower particle number concentration hemispheric (LC) from N to SSW in clockwise (6550 ± 780) cm^{-3}.

Annual cycle allowed to conclude that the increase or decrease of 1 cm^{-3} of N_{NUC} was related to opposite trend of 0.5 cm^{-3} of N_{ACC} and, moreover, that, the relation between monthly N_{NUC}&N_{ACC} was highly correlated with R=0.66. It could be explained because of the presence of large particles from desert dust air mass resulted in an aerosol aging and an increase of N_{ACC}. It produced a large surface area concentration which favoured the condensation process onto pre-existing aerosols and suppressed the nucleation events (decreasing N_{NUC}). This anti-correlation between both modal concentrations produced a weak seasonal evolution of N_T.

586 ~~On the other hand,~~ A trend of increasing the N_{AIT} is observed with a rate of 1150 cm^{-3} $year^{-1}$. It is
587 not possible to conclude the reason for this ~~conduct because many more years with~~ increase
588 ~~measurements are necessary.~~ without additional measurements

589

590 ## Acknowledgement

591 This work has been supported by the Spanish Ministry for Science and Innovation (MICINN)
592 by means of project CLIMARENO- CGL2008-05939-C03-03/CLI. Authors would like to
593 express their gratitude to the European Union (6th framework EUSAAR – RII3-CT-2006-
594 026140) for providing technical support

595

596 ## References

597 Adame, J.A., Lozano, A., Bolívar, J.P. De la Morena, B.A., Contreras, J., and Godoy, F.:
598 Behaviour, distribution and variability of surface ozone at an arid region in the south of
599 Iberian Peninsula (Seville, Spain), Chemosphere, 70, 841-849, 2008.

600 Adame, A. A., Serrano, E., Bolivar, J. P. and De la Morena, B.A.: On the tropospheric ozone
601 variations in a coastal area of Southwestern Europe under a Mesoscale Circulation. Journal of
602 Applied Meteorology and Climatology, doi: 10.1175/2009JAMC2097.1, 2010

603 Antilla, P., Rissanen, T., Shimmo, M., Kallio, M., Hyötyläinen, T., Kulmala, M. and
604 Riekkola, M.-L.: Organic compounds in atmospheric aerosols from a Finish coniferous forest,
605 Boreal Environment Research, 10, 371 – 384, 2005.

606 Birmili, W., Stratmann, F., Wiedensohler, A., Covert, D., Russell, L.M. and Berg, O:
607 Determination of differential mobility analyzer transfer functions using identical instruments
608 in series, Aerosol Sci. Tech., 27, 215-223, 1997.

609 Birmili, W., Wiedensohler, A., Heintzenberg, J. and Lehmann, K.: Atmospheric particle
610 number size distribution in central Europe: statistical relations to air masses and meteorology,
611 J. Geophys. Res., 106, 32005-32018, 2001.

612 Birmili, W., Berresheim, H., Dülmer, C.P., Elste, T., Gilge, S., Wiedensohler, A., and Uhrner,
613 U.: The Hohenpeissenberg Aerosol Formation Experiment (HAFEX): a Long-term Study
614 Including Size-resolved Aerosol, H_2SO_4, OH, and Monoterpenes Measurements, Atmos.
615 Chem. Phys., 3, 361-376, 2003.

616 Buzorius, G., Kannik, U, Aalto, P., Dal Maso, M., Nilsson, E.D., Lehtinen, K. E. J., and
617 Kulmala, M.: On particle formation prediction in continental boreal forest using
618 micrometeorological parameters, J. Geophys., Res., vol. 108 (D13), 4377,
619 doi:10.1029/2002JD002850, 2003.

620 Cachorro, V.E., Toledano, C., Prats, N., Sorribas, M., Mogo, S., Berjón, A., Torres, B., Rodrigo,
621 R., De Frutos, A.M., De la Rosa, J., and De la Morena, B.A: The strongest desert dust intrusion
622 mixed with smoke over the Iberian Peninsula registered with sun-photometry, J. Geophys.
623 Res., 113, D14S04, doi:10.1029/2007JD009582, 2008.

624 Charlson, R.J., Lovelock, J.E., Andreae, M.O., and Warren, S.G.: Oceanic phytoplankton,
625 atmospheric sulphur, cloud albedo and climate, Nature, 326, 655-661, 1987.

626 Charlson, R.J., and Wigley, T.M.L.: Sulphate aerosol and climate change, Sci. Am., 270, 48-
627 57, 1994.

628 Córdoba-Jabonero, C., Sorribas, M., Guerrero-Rascado, J.L., Adame, J.A., Hérnandez, Y.,
629 Lyamani, H., Cachorro, V., Gil, M., Alados-Arboledas, L., Cuevas, E. and De la Morena, B.:
630 Synergetic monitoring of Saharan dust plumes and potential impact on surface: a case of
631 study of dust transport from Canary Islands to Iberian Peninsula. Atmos. Chem. Phys.
632 Discuss., 10, 27015-27074, doi:10.5194/acpd-10-27015, 2010.

633 Dingenen, V., Putaud, J.P., Martins-Dos Santos, S., and Raes F.: Physical aerosol properties
634 and their relation to air mass origin at Monte Cimone (Italy) during the first MINATROC
635 campaign, Atmos. Chem. Phys., 5, 2203-2226, 2005.

636 Heintzenberg, J., Covert, D.C., and Dingenen, R.V: Size distribution and chemical
637 composition of marine aerosols: a compilation and review, Tellus, 52B, 1104 – 1122, 2000.

638 Ieda, T., Kitamori, Y., Mochida, M., Hirata, R., Hirano, T., Inulai, K., Fijinuma, Y., and
639 Kawamura, K.: Diurnal variations and vertical gradients of biogenic volatile and semi-volatile
640 organic compounds at the Tomakomai larch forest stations in Japan, Tellus, 59B, 177-186,
641 2006.

642 IPCC (Intergovermental Panel of Climate Change), available at: http://www.ipcc.ch/, 2007.

643 Janhäll, S., Andreae, M. O., and Pöschl, U.: Biomass burning aerosol emissions from
644 vegetation fires: particle number and mass emission factors and size distribution. Atmos.
645 Chem. Phys., 10, 1427-1439, 2010.

646 Knutson, E.O., and Whitby, K.T.: Aerosol classification by Electric Mobility: Apparatus,
647 Theory and Applications, J. Aerosol Sci., 6, 443 – 451, 1975.

648 Kulmala, M., Hämeri, K., Aalto, P.P., Mäkelä, J.M., Pirjola, L., Douglas, N., Buzorius, G.,
649 Rannik, Ü, Dal Maso, M., Seidl, W., Hoffman, T., Janson, R., Hansson, H.-C., Viisanen, Y.
650 Laaksonen, A., and O'Dowd, C.D.: Overview of the international project on biogenic aerosol
651 formation in the boreal forest (BIOFOR), Tellus, 53B, 324-343, 2001.

652 Kulmala, M., Vehkamäki, H., Petäjä, T., Dal Maso, M., Lauri, A., Kerminen, V.-M., Birmili,
653 W., and MecMurry, P.H.: Formation and growth rates of ultrafine atmospheric particles: a
654 review of observations, Aerosol Sci. Tech., 35, 143 – 176, 2004.

655 Laakso, L., Hussein, T., Aarnio, P., Komppula, M., Hiltunen, V., Viisanen, Y., and Kulmala
656 M.: Diurnal and annual characteristics of particle mass and number concentrations in urban,
657 rural and Arctic environments in Finland, Atmos. Environ., 37, 2629-2641, 2003.

658 Liu, S., Hu, M., Wu, Z., Wehner, B., Wiedensohler, A., and Cheng, Y.: Aerosol number size
659 distribution and new particle formation at a rural/coastal site in Pearl River Delta (PRD) of
660 China, Atmos. Environ., 42, 6275-6283, 2008.

661 Ma, Y., and Lyons, T.L.: Recirculation of coastal urban air pollution under a synoptic scale
662 thermal trough in Perth, Western Australia, Atmos. Environ., 37, 443-454, 2003.

663 Mahajan, A., S., Sorribas, M., Gómez Martín, J.C., MacDonald, S. M., Gil, M., Plane, J. M.
664 C., and Saiz-Lopez, A.: Concurrent observations of atomic iodine, molecular iodine and
665 ultrafine particles in a coastal environment, Atmos. Chem. Phys. Discuss., 10, 27227-27253,
666 2010.

667 Mogo, S., Cachorro, V.E., Sorribas, M., De Frutos, A.M., and Fernández, R.: Measurements
668 of continuous spectra of atmospheric absorption coefficients from UV to NIR via optical
669 method, Geophys. Res. Lett., 32, L13811, doi:10.1029/2005GL022938, 2005.

670 Mogo, S., Cachorro, V.E., De Frutos, A. M., De la Rosa, J., and Sorribas, M.: Comparing
671 surface measurement of black carbon and columnar AERONET inferred contents during the
672 "El Arenosillo 2004 summer campaign". Opt. Pura Apl., 43 (1), 49 - 55, 2010.

673 Niemi, J.V., Tervahattu, H., Vehkamäki, H., Kulmala, M., Koskentalo, T., Sillanpää, M., and
674 Rantamäki M.: Characterization and source identification of a fine particle episode in Finland,
675 Atmos. Environ., 38, 5003-5012, 2004.

676 Pey, J., Querol, X., De la Rosa, J., Gonzalez-Castanedo, Y., Alastuey, A., Gangoiti, G.,
677 Sánchez de la Campa, A., Alados-Alboledas, L., Sorribas, M., Pio, C., Cachorro, V., Piñeiro,
678 M., López-Mahia, P., and García-Gacio, D.: Characterization of a long range transport
679 pollution episode affecting PM in SW Spain, J. Environ. Monitor., doi: 10.1039/b809001g,
680 2008.

681 Prats, N., Cachorro, V.E., Sorribas, M., Mogo, S., Berjón, A., Toledano, C., De Frutos, A.M.,
682 De la Rosa, J., Laulainen, N., and De la Morena, B.A.: Columnar aerosol optical properties
683 during El Arenosillo 2004 summer campaign, Atmos. Environ., 42, 2643-2653, 2008.

684 Querol, X., Alastuey, A., Rodríguez, S., Viana, M.M., Artíñano, B., Salvador, P., Mantilla, E.,
685 García do Santos, S., Fernández Patier R., De la Rosa, J., Sanchez de la Campa, A.,
686 Menéndez, M., Gil, J.J.: Levels of particulate matter in rural, urban and industrial sites in
687 Spain. Science of Total Environment, 334-335, 359-376, 2004.

688 Querol, X., Alastuey, A., Moreno, T., Viana, M. M., Castillo, S., Pey, J., Rodríguez, S.,
689 Artiñano, B., Salvador, P., Sánchez, M., García Dos Santos, S., Herce Garraleta, M.D.,
690 Fernández-Patier, R., Moreno-Grau, S., Negral, L., Minguillon, M.C., Monfort, E., Sanz,
691 M.J., Palomo-Marín, R., Pinilla-Gil, E., Cuevas, E., De la Rosa, J. and Sánchez de la Campa,
692 A.: Spacial and temporal variations in airborne particulate matter (PM_{10} and $PM_{2.5}$) across
693 Spain 1999-2005, Atmos. Environ, 42, 3964-3979, 2008.

694 Reid, J.S., Koppmann, R., Eck, T.F. and Eleuterio, D.P.: A review of biomass burning
695 emissions part II: intensive physical properties of biomass burning particles, Atmos. Chem.
696 Phys., 5, 799-825, 2005.

697 Rodríguez, S., Dingenen, R. V., Putaud ,J.-P, Santos, S. M.-D, and Roselli D.: Nucleation and
698 growth of new particles in the rural atmosphere of Northern Italy-relationship to air quality
699 monitoring, Atmos. Environ., 39, 6734-6746, 2005.

700 Sánchez de la Campa, A.M., Pio, C., De la Rosa, J., Querol, X., Alastuey, A., González-
701 Castanedo, Y.: Characterization and origin of EC and OC particulate matter near the Doñana
702 National Park (SW Spain), Environ. Res., 109, 671-681, 2009.

703 Sheridan, P.J., Delene, D.J., and Ogren, J.A.: Four years of continuous surface aerosol
704 measurements from the Department of Energy's Atmospheric Radiation Measurement
705 Program Southern Great Plains Cloud and Radiation Testbed site, J. Geophys. Res., 106, 18,
706 20735-20747, 2001.

707 Sorribas, M., Cachorro, V.E., Adame, J.A., Wenner, B., Birmili, W., Widensohler, A.:
708 Submicrometer aerosol size distributions in southwest-ern Spain: relation with meteorological
709 parameters, Proc. 17th Int. Conf. on Nucleation and Atmospheric Aerosols, Galway, Ireland,
710 829-833, 2007.

711 Sorribas, M.: Medida y Caracterización del Aerosol Atmosférico en un Ambiente Rural y
712 Costero del Suroeste de Europa. La distribución Numérica de Tamaños en el Rango Sub-
713 micrométrico. (Measurement and characterization of Atmospheric aerosol in a rural and
714 coastal environment. Sub-micron particle number size distribution in Southwestern Europe).
715 Ph. D. thesis, University of Valladolid, Valladolid, Spain, 350 pp. [Available online at
716 http://sites.google.com/site/marsorribas/], 2008.

717 Ström, J., Umegard, J., Torseth, K., Tunved, P., Hansson, H.-C., Holmén, K., Wismann, V.,
718 Herber, A. and König-Langlo.: One year of particle size distribution and aerosol chemical
719 composition measurements at the Zeppelin Station, Svalbard, March 2000-March 2001,
720 Physics and Chemistry of the Earth, 28, 1181-1190, 2003.

721 Su, Y.F., Cheng, Y.S., Newton, G.J., and Yeh, H.C.: Counting efficiency of the TSI Model
722 3020 Condensation Nucleus Counter, Aerosol Sci. Techn., 12, 1050-1054, 1990.

723 Takemura, T., Nakajima, T., Dubovic, O., Holben, B.N., and Kinne, S.: Single-scattering
724 albedo and radiative forcing of various aerosol species with a global three-dimensional model,
725 J. Climate, 15, 4, 333 – 352, 2002.

726 Toledano, C.: Climatología de los aerosoles mediante la caracterización de propiedades
727 ópticas y masas de aire en la estación 'El Arenosillo' de la red AERONET. (Aerosol
728 Climatology through the characterization of optical properties and air masses at El Arenosillo
729 station of the AERONET network). Ph. D thesis, University of Valladolid, Valladolid, Spain,
730 239 pp, [Available online at http://goa.uva.es/~toledano/], 2005.

731 Toledano, C., Cachorro, V.E., Berjón, A., De Frutos, A.M., Sorribas, M., De la Morena, B.A.,
732 and Goloub, P.: Aerosol optical depth and Ángstrom exponent climatology at El Arenosillo
733 AERONET site (Huelva, Spain), Q. J. R. Meteorol., Soc., 133, 795-807, 2007a.

734 Toledano, C., Cachorro, V.E., De Frutos, A.M., Sorribas, M., Prats, N., and De la Morena,
735 B.A.: Inventory of African desert dust events over the southwestern Iberian Peninsula in
736 2000-2005 with an AERONET Cimel Sun photometer, J. Geophys. Res., 112, D21201,
737 doi:10.1029/2006JD008307, 2007b.

738 Tunved, P., Hansson, H.-C., Kulmala, M., Aalto, P., Viisanen, Y., Karlsson, H., Kristensson,
739 A., Swietlicki, E., Dal Maso, M., Ström, J., and Komppula, M: One year boundary layer
740 aerosol size distribution data from five nordic background stations, Atmos. Chem. Phys., 3,
741 2183 – 2205, 2003.

742 Venzac, H., Sellegri, K., Villani, P., Picard, D. and Laj, P. : Seasonal variation of aerosol size
743 distributions in the free troposphere and residual layer at the puy de Dôme station, France.
744 Atmos. Chem. Phys., 9, 1465-1478, 2009.

745 Vergaz, R., Cachorro, V. E., De Frutos A. M., Vilaplana, J.M., and De la Morena, B.A.:
746 Columnar characteristics of aerosols by spectroradiometer measurements in the maritime area
747 of the Cadiz Gulf (Spain), Int. J. Climatol., 25, 1781 – 1804, 2005.

748 Willeke, K., and Baron, P.A.: Aerosol measurements principles, techniques and applications.
749 Van Nostrand Reinhold, New York, USA, pp. 143-195, 1993.

750 Wright, M.E., Atkinson, D.B., Ziemba, L., Griffin, R., Hiranuma, N., Brooks, S., Lefer, B.,
751 Flynn, J., Perna, R., Rappengluck, B., Luke, W., Kelley, P.: Extensive aerosol optical
752 properties and aerosol mass related measurements during TRAMP/TexAQS 2006-
753 Implications for PM compliance and planning, Atmos. Environ, 44, 33, 4035-4044, 2010.

	N_{Total} (cm^{-3})	Nucleation Mode (cm^{-3})	Aitken Mode (cm^{-3})	Accumulation Mode (cm^{-3})
	Entire period of study			
Mean	8660	2830	4110	1720
STD	6740	4500	3220	1120
Max non-event	83222	68938	35171	6750
Min	140	12	60	32
Median	7090	1470	3260	1530
10^{th} percentile	3250	340	1370	480
90^{th} percentile	15450	6800	7730	3160
	During the mixed event			
Mean	27620	13320	12020	2270
STD	27060	21900	8560	1240
Max	188700	152340	37310	14950
Min	2220	13	670	600
Median	22440	7240	9800	2000
10^{th} percentile	6520	900	3770	1020
90^{th} percentile	47790	24500	25870	3580

Table 1. Statistic of the total and modal concentration for 1-hour year data series and only for the mixed event (desert dust episode plus forest fire) happened during 27 July – 4 August 2004.

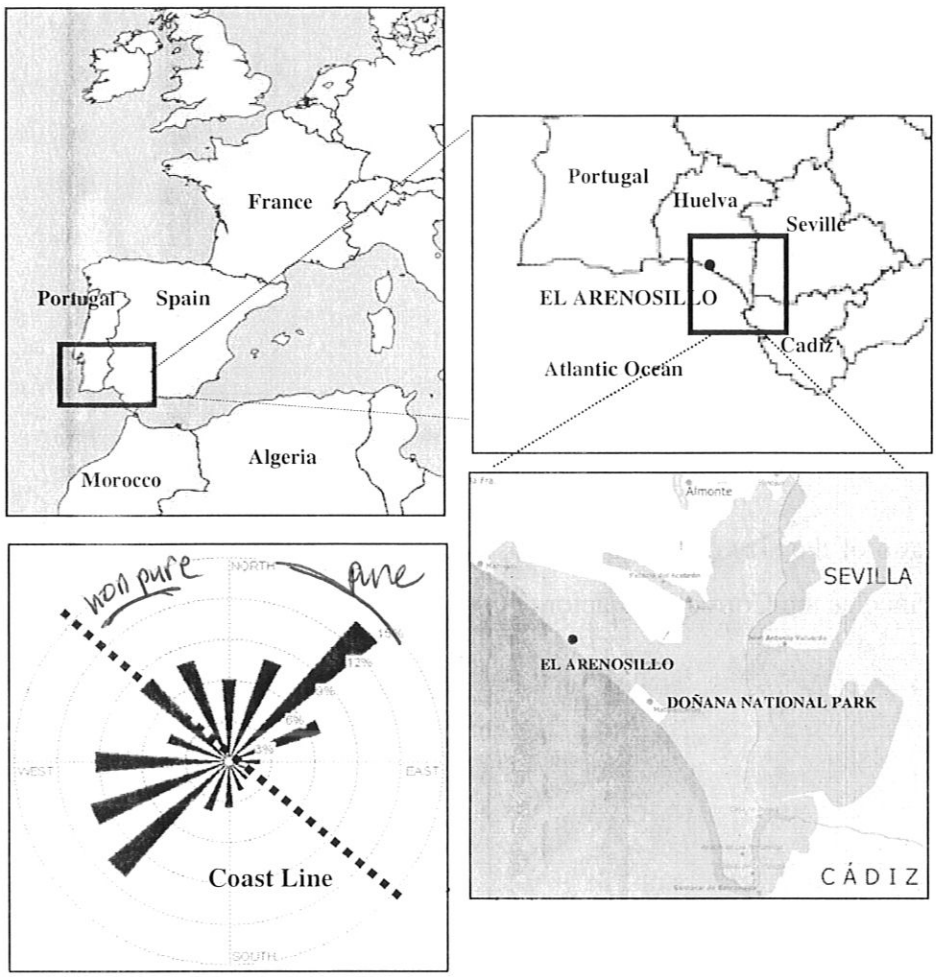

Figure 1. Map of Iberian Peninsula highlighting the location of El Arenosillo Station, the (15/07/04 – 31/07/06) wind rose and the coastal line.

put an arc on windrose indicate pure & non pure

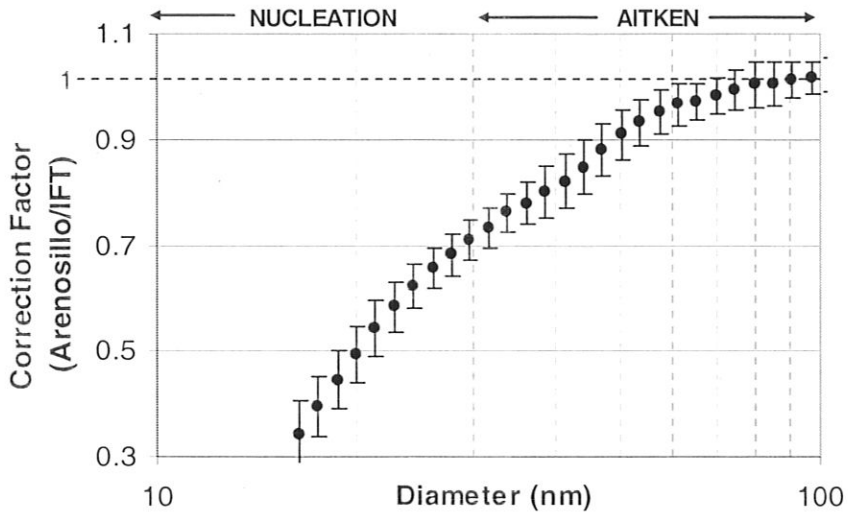

Figure 2. Ratio of the size distribution measured by the SMPS-El Arenosillo and the DMPS-IfT. It is defined as the Correction Factor (FC).

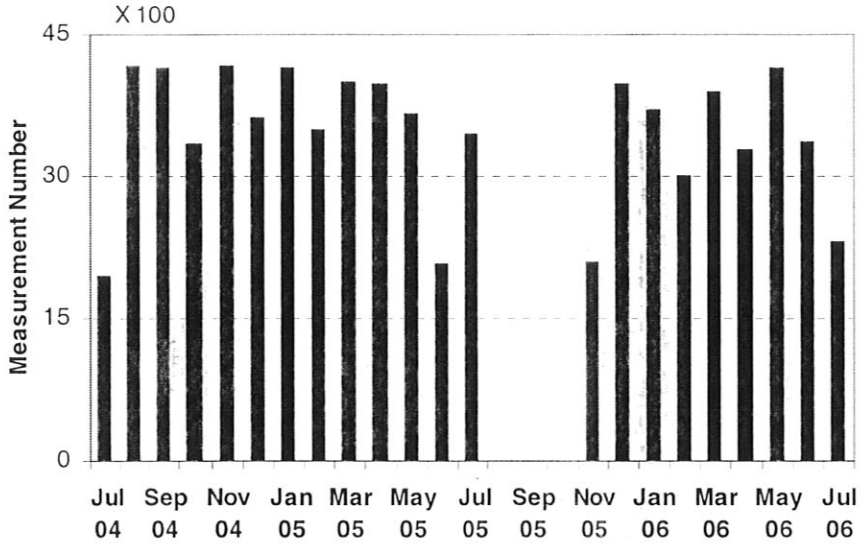

Figure 3. Number of the particle number size distributions per month at El Arenosillo Station from the 10-min data-base used for the analysis.

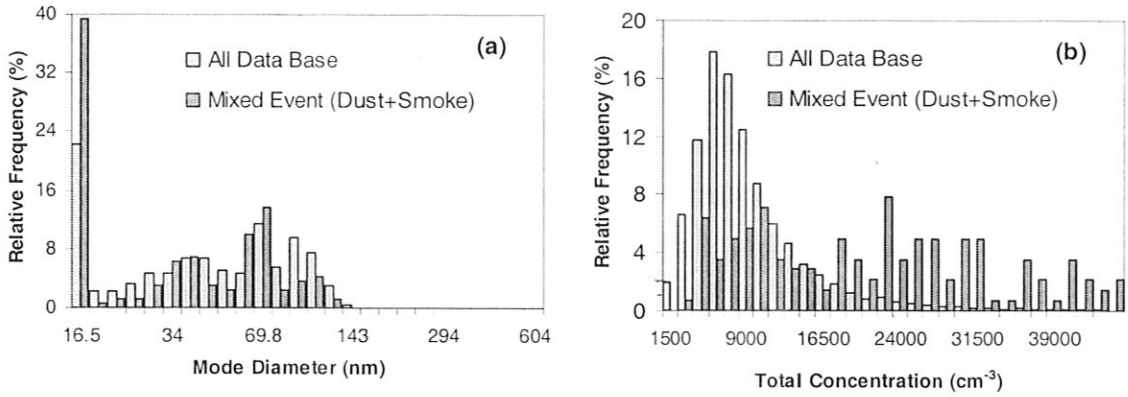

Figure 4. The relative occurrence frequency of (a) mode diameter and (b) total particle concentration of 1-hour data for the entire period of study and during the special mixed event.

Change axes log scale
make major ticks more obvious so can figure out
how to line up numbers w/ bars

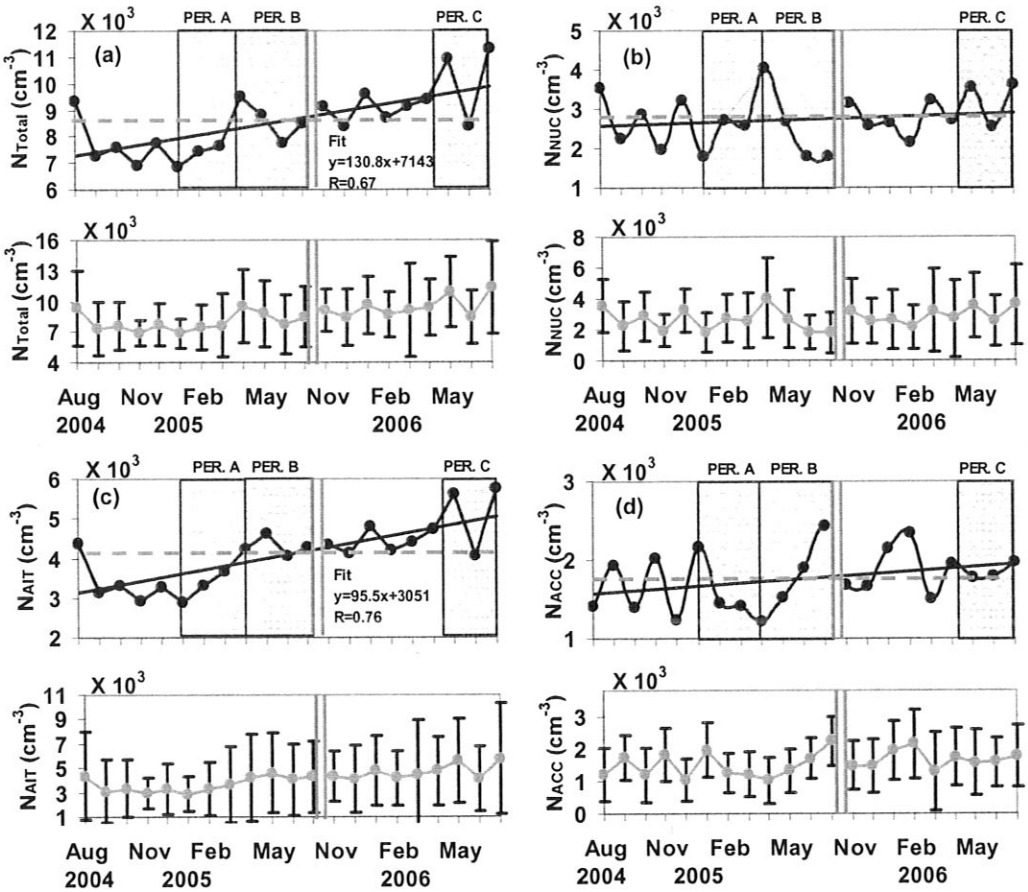

Figure 5. Annual cycle with monthly mean levels for (a) N_T, (b) N_{NUC}, (c) N_{AIT} and (d) N_{ACC}. The mean values are also indicated (dashed grey line). 10th and 90th percentiles are indicated in subplots.

rearrange

make major ticks more obvious

or put percentiles on main plot

say what black line is

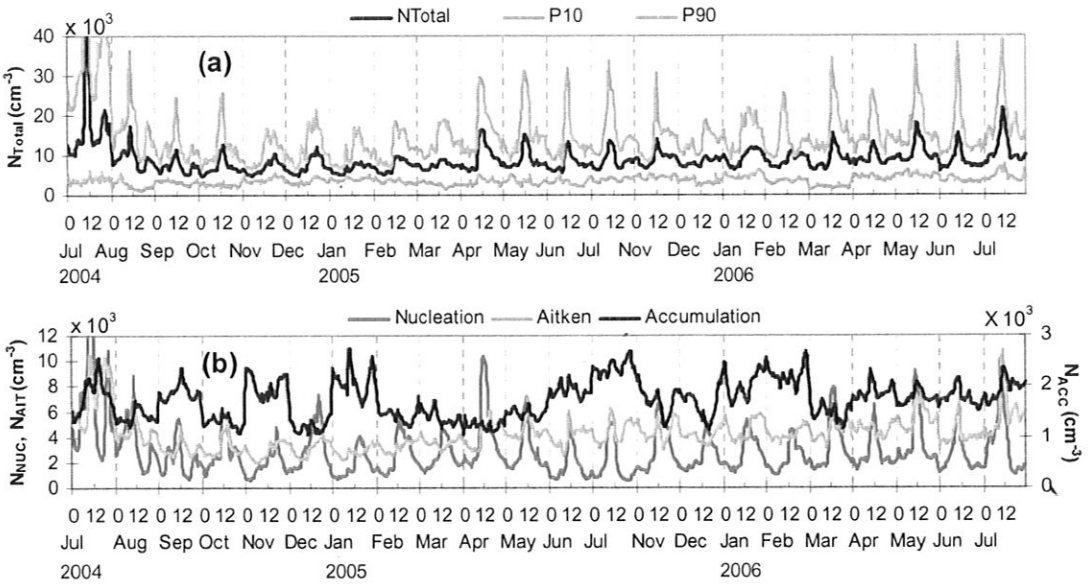

Figure 6. Daily mean cycles per month of (a) total concentration (N_T) (blank line) with the 10th and 90th percentiles (grey lines) (b) and concentrations for nucleation (N_{NUC}), Aitken (N_{AIT}) and accumulation (N_{ACC}) modes.

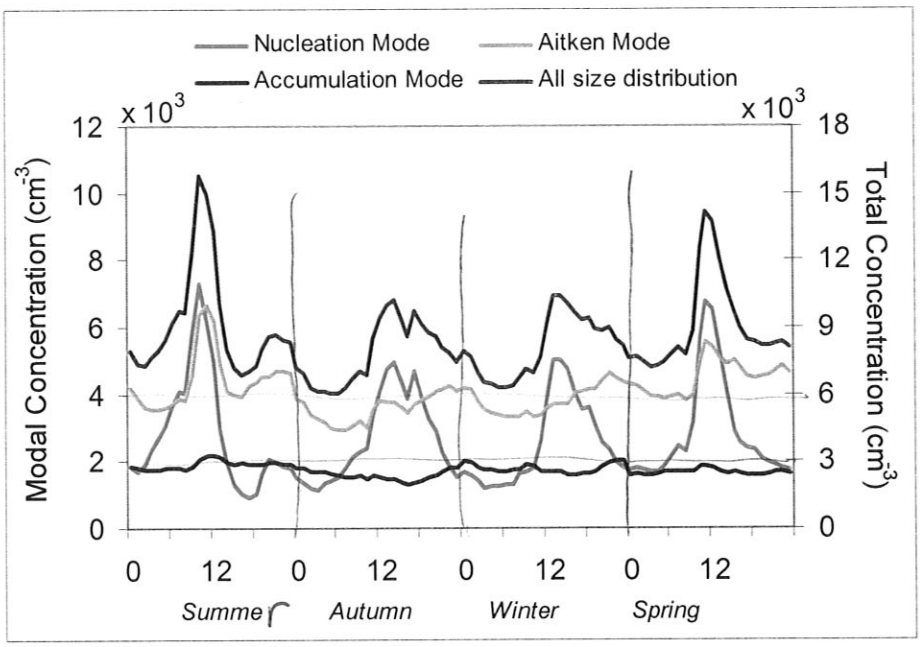

Figure 7. Daily mean cycles of the total and nucleation, Aitken and accumulation mode concentrations per season, July-September (summer), October-December (autumn), January-March (winter) and April-June (spring).

vertical lines to delineate season

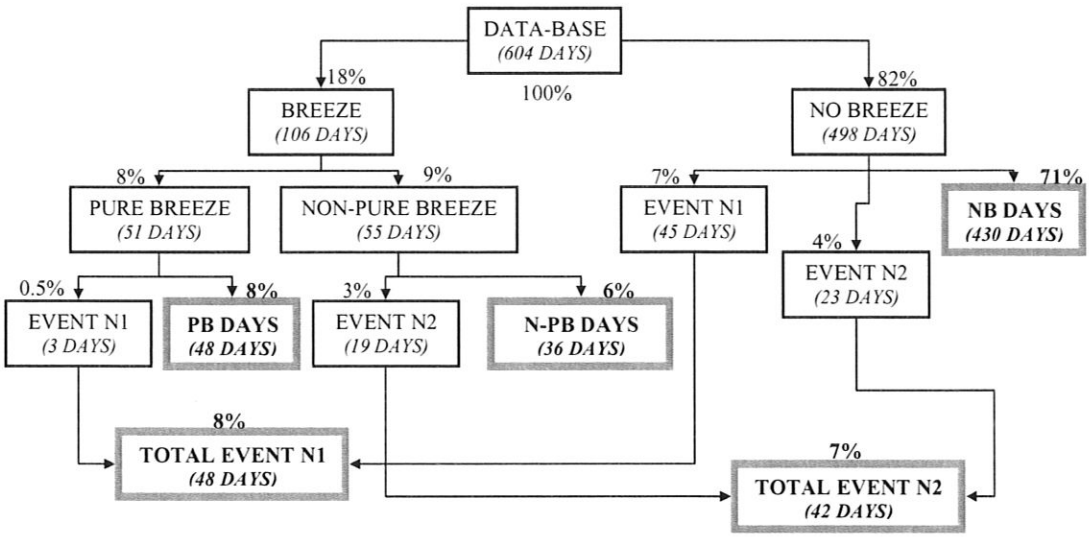

Figure 8. Representative day's segregation by means of sea-land breezes (pure and non-pure) days and nucleation events (N_1 and N_2).

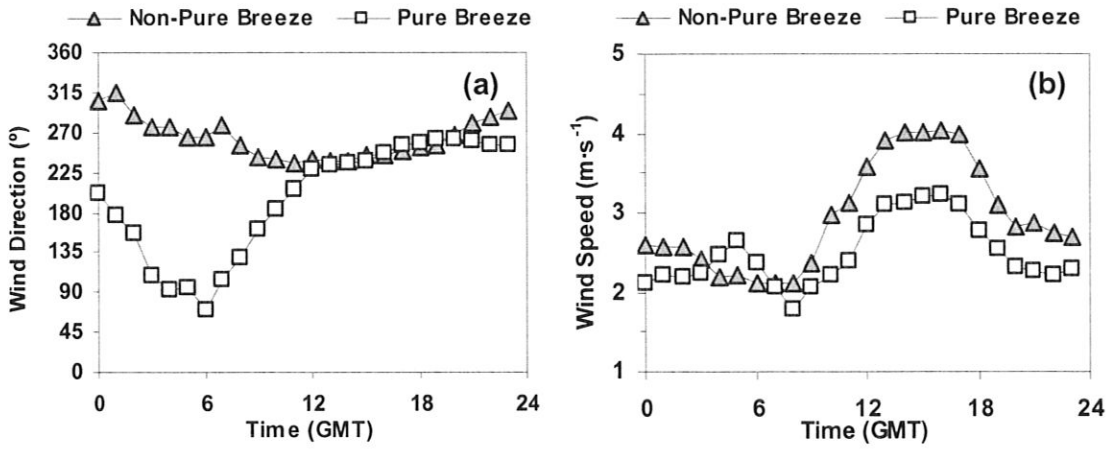

Figure 9. Daily evolution of mean (a) wind direction and (b) wind speed for pure (51 days) and non-pure (55 days) breezes patterns during data-base used for this analysis.

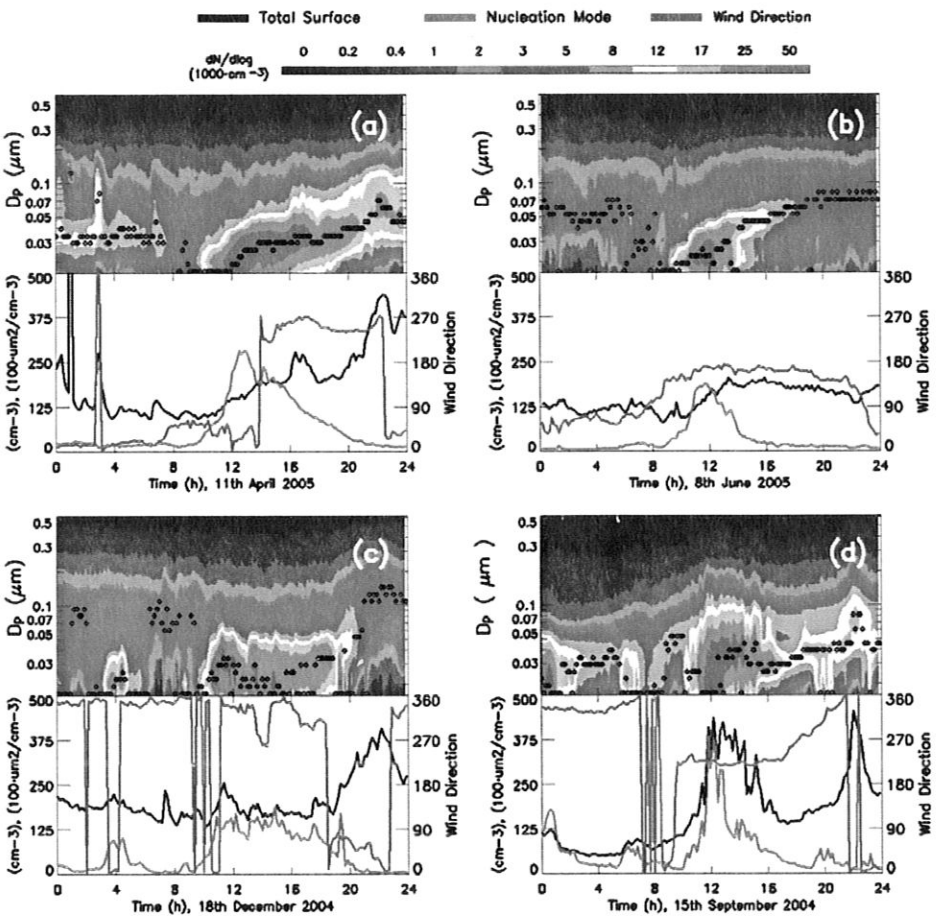

Figure 10. Daily evolutions of the particle number size distribution at El Arenosillo Station, during (a) 11 April 2005, (b) 8 June 2005, (c) 18 December 2004 and (d) 15 September 2004. Total surface (black line), concentration for nucleation mode (red line), wind direction (green line) and mode diameter (black diamonds) are also represented.

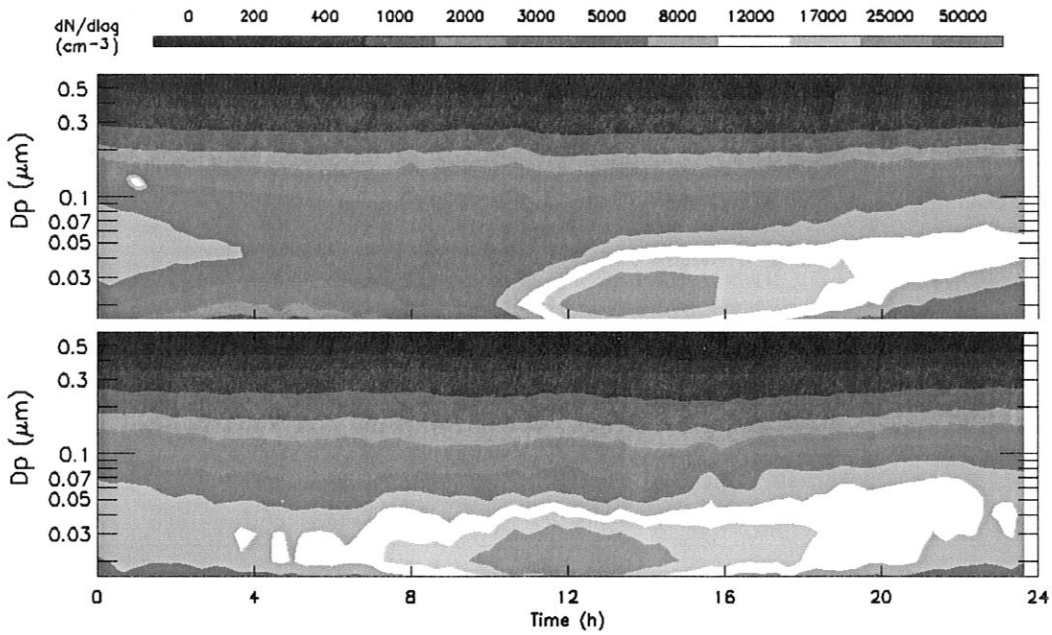

Figure 11. Mean particle size distribution for new particle formation with (up) wind blowing from NE (Event N_1, 48 days) and (down) blowing from NW (Event N_2, 42 days) at El Arenosillo Station.

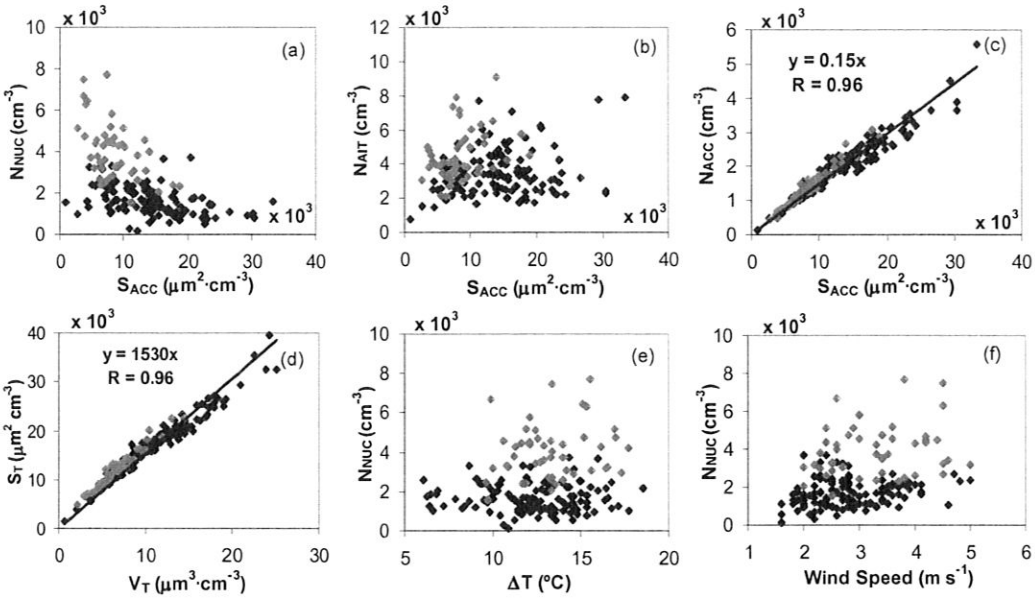

Figure 12. 24-h averaged of several submicron aerosol physical properties and meteorological parameters at El Arenosillo station. Add what colors are to caption

Red = N_1

Black = daily mean

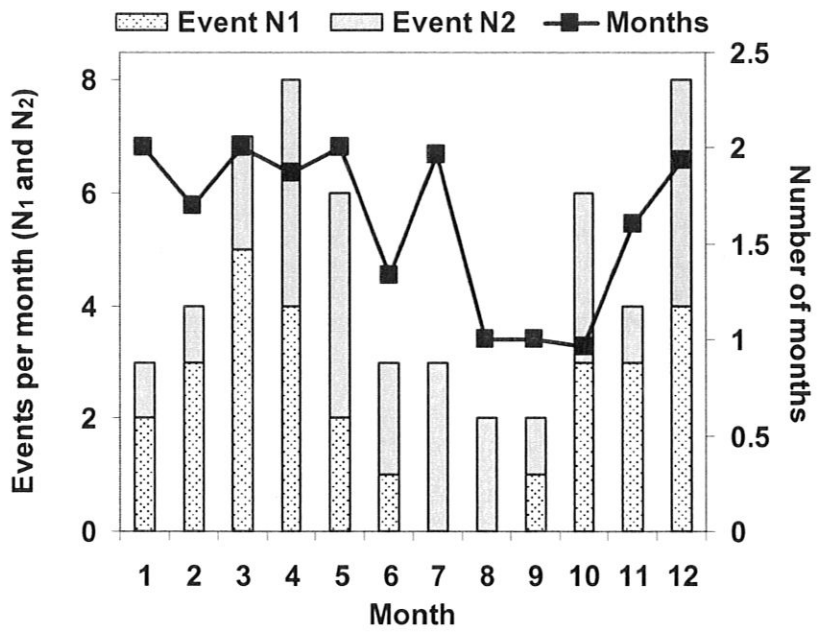

Figure 13. Percent of days per month with Event N_1 and Event N_2.